2020-08-03

Loads on a Point-Absorber Wave Energy Converter in Regular and Focused Extreme Wave Events

Katsidoniotaki, E

10.1115/omae2020-18639
Volume 9: Ocean Renewable Energy
American Society of Mechanical Engineers

Proceedings of the ASME 2020 39th International Conference on Ocean, Offshore and Arctic Engineering
OMAE2020
June 28-July 3, 2020, Fort Lauderdale, FL, USA

OMAE2020-18639

LOADS ON A POINT-ABSORBER WAVE ENERGY CONVERTER IN REGULAR AND FOCUSED EXTREME WAVE EVENTS

Eirini Katsidoniotaki[1]*, Edward Ransley[2], Scott Brown[2], Johannes Palm[3], Jens Engström[1], and Malin Göteman[1]
[1] Department of Electric Engineering, Uppsala University, Uppsala, Sweden
[2] University of Plymouth, Plymouth, UK
[3] Chalmers University, Gothenburg, Sweden

ABSTRACT

Accurate modeling and prediction of extreme loads for survivability is of crucial importance if wave energy is to become commercially viable. The fundamental differences in scale and dynamics from traditional offshore structures, as well as the fact that wave energy has not converged around one or a few technologies, implies that it is still an open question how the extreme loads should be modeled. In recent years, several methods to model wave energy converters in extreme waves have been developed, but it is not yet clear how the different methods compare. The purpose of this work is the comparison of two widely used approaches when studying the response of a point-absorber wave energy converter in extreme waves, using the open-source CFD software OpenFOAM. The equivalent design-waves are generated both as equivalent regular waves and as focused waves defined using NewWave theory. Our results show that the different extreme wave modeling methods produce different dynamics and extreme forces acting on the system. It is concluded that for the investigation of point-absorber response in extreme wave conditions, the wave train dynamics and the motion history of the buoy are of high importance for the resulting buoy response and mooring forces.

INTRODUCTION

As many wave energy concepts are reaching a stage where offshore experiments are conducted or full-scale devices are being constructed, increasing attention is being paid to prediction of design loads and dynamics in harsh offshore conditions and in extreme waves. Underestimation of loads may lead to component failure, whereas overestimation could result in increased structural costs and possibly reduced performance in operational mode. As such, the estimation of extreme loads largely dictates the cost of wave energy [1, 2], which makes it one of the most important challenges for wave energy development. Since physical experiments are both expensive and difficult to carry out, numerical simulations provide a necessary tool in the design process. Potential flow methods are not capable of capturing the non-linear dynamics in extreme waves [3, 4]. Computational resources in terms of high performing computer clusters are becoming increasingly accessible, which enables numerical modeling with high-fidelity computational fluid dynamics (CFD) methods.

In traditional offshore engineering, standards and recommended practices have long since been established with regards to how to design the extreme wave conditions when studying design loads and survivability. For wave energy converters (WECs), however, identifying which environmental conditions lead to the maximal loads or component failures is not a trivial problem. The small scale and the dynamics of WECs lead to ultimately different systems than in traditional offshore engineering. For example, WECs are often designed to operate in resonance with waves whereas offshore platforms and ships are designed to avoid resonance. The survivability of WECs in extreme waves is a critical issue for wave energy utilizations since

*Corresponding author: eirini.katsidoniotaki@angstrom.uu.se

it can lead to fatal consequences for the system operation, however, it is not always the largest wave that produces the largest loads [2, 5–7]. One of the few design standards that exists for wave energy is developed by The International Electrotechnical Commission (IEC). It recommends that the significant wave height recurring every 50-years on average, $H_{s(50)}$, is to be used when designing reliable wave energy converters and evaluating their offshore risks [8].

However, even after the extreme wave characteristics have been decided in terms of a wave contour, it is far from straightforward how the maximal load for a device should be identified, and different methods exist [9]. A standard approach from offshore engineering is to study the device response in a long time series of irregular waves. Typically, a 3-hour wave train is required in full scale for statistical convergence [10], but this is not feasible for a well-resolved CFD simulation due to the high computational costs associated with this method, and low-fidelity methods such as linear potential flow methods neglect non-linear effects, viscosity, and other aspects that are of high importance for the dynamics and performance of the device in steep waves. For this reason, methods to study the WEC in equivalent design waves have been developed in recent years. Presently, both regular and focused waves are commonly used as design waves [3, 4, 11–14], but the reliability of the methods for predicting extreme loads is still an open question, along with how the different methods compare. This is the topic of the current paper.

There have been a number of previous studies aimed at comparing extreme loads. NewWave theory is one approach which has become the industry standard for modeling extreme wave interactions with offshore structures [15]. In [16], a focused wave was designed using NewWave theory and extreme loads on a CETO WEC were studied using a linear as well as a CFD method, and it was found that the linear model overestimated the load and motion of the device. In [5], mooring loads on a single taut moored floating WEC were studied experimentally in focused waves, generated using NewWave theory. It was concluded that for dynamical bodies, the motion history of the float has a large impact on the mooring loads, which indicates that single focused waves may not accurately be used to compute extreme mooring loads. Another approach to model extreme waves as focused wave events is the most likely extreme response (MLER) method, which takes into account the response of the structure. It was used in [3] to define equivalent focused waves to five extreme states along the 100-year contour at the Humboldt Bay, California, and the device response was then studied in the resulting wave profile using both WEC-Sim and a CFD model. In [17], both regular and focused waves were used to study the extreme wave loading on a Triton WEC, both experimentally in scale 1:30 and numerically with a midfidelity and a CFD model. When comparing the CFD models for the regular and focused waves, they found that the former showed up to 34% difference from the experimental design load response, whereas the latter produced a result within 17% of the experimental data. In [14], a WEC-Sim model was compared with a STAR-CCM+ CFD model for a focused wave obtained using NewWave theory, and the overall responses predicted by the two models compared well, and were on average within 5% from each other. This is in contrast to the results of [18], where the dynamics predicted by a high-fidelity CFD method gave a better agreement with experimental data than linear-based models.

As is clear from the papers discussed above, there are uncertainties in determining extreme loads on WECs, and determining those is of crucial importance for the development of wave energy technology. Along with the difficulties in translating existing methods from traditional offshore industries due to the different scale, dynamics of WECs and approaches for extreme wave events modelling, the lack of convergence of wave energy devices to one or a few technologies also affects. Hundreds of different technologies exist, with different behaviour in extreme waves, implying that results for one WEC concept cannot be directly translated to another.

In this paper, a CFD model for a point-absorber WEC is used to study the behaviour in different extreme waves. Point-absorbers are one of the most studied wave energy concepts, and the present device developed by Uppsala University is a good example of this technology. The WEC consists of a buoy connected to a direct-driven linear generator with limited stroke length. To allow for more straightforward comparison, two of the sea states studied in [3] have been selected, and represent extreme sea states along the 100-year contour at the Humboldt Bay, California. Two different methods are used to define and model the equivalent extreme waves: regular waves with wave height $H = 1.9 \cdot H_s$, and focused waves defined using NewWave theory. The different extreme wave approaches are compared and the line force and dynamics of the WEC in the different extreme wave conditions are evaluated.

The paper is divided as follows. In the next section we present and discuss the methods of the paper: the wave energy converter system, the extreme wave models and the numerical modeling. The results first show mesh convergence, and then discuss the WEC dynamics and forces in the extreme wave events. Conclusions are presented and discussed in the last section.

METHOD

Wave energy converter

The wave energy converter (WEC) studied in this paper is based on the wave energy concept developed at Uppsala University [19]. The concept has been realized in fullscale WECs tested in several offshore campaigns [20]. The WEC consists of a cylinder buoy connected to a direct-driven linear generator. The translator moves vertically within the stator with a limited stroke length, see Fig. 1. The translator is pulled upwards by the motion of the buoy, and downwards by its own weight. End-stop springs

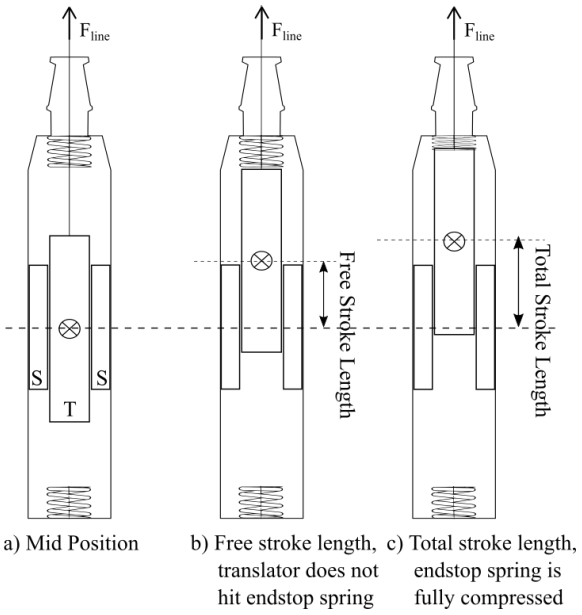

FIGURE 1: THE DIRECT-DRIVEN LINEAR GENERATOR HAS A LIMITED STROKE LENGTH. FIGURE ADAPTED FROM [22].

are attached at the upper and lower end-stops, and will be compressed when the wave height exceeds the stroke length. This two-body system is able either for coupled motion or moving separately, depending on the connection line tension. The translator inside the power take-off (PTO) system has a limited stoke length. Once the upper end-stop spring is fully compressed, the connection line acts as an elastic mooring line adding a further restraint force in the system. When the translator hits the lower end-stop spring the line force slacks and the two-body system motion is uncoupled. During extreme waves, it has been seen that damaging peak line forces can be avoided by increasing generator damping, which slows down the motion of the translator [21]. In this paper however, a constant generator damping is applied. The dimensions and parameter values for the WEC are given in Table1.

Extreme wave modelling

As was discussed in the introduction, there is a limited amount of design practices and technical specifications regarding WECs design and their evaluation on extreme wave conditions. A sea state is a stochastic phenomenon and the definition of the design-wave is not a straightforward process. There are three common approaches for design-wave definition, as reviewed in [9]: irregular wave trains, equivalent regular waves and focused waves based on sea state parameters. For the purposes of high-fidelity simulations, an irregular wave time series is computational expensive, since time frames of three hour realizations of the sea state are generally recommended. Alternatively, the concept of equivalent design-wave approaches is applicable for short-period CFD simulations. In this paper, both regular and focused wave events are applied and compared.

TABLE 1: DIMENSIONS OF THE STUDIED WAVE ENERGY CONVERTER.

Parameter	Value
Buoy radius	1.7 m
Buoy height	2.12 m
Buoy draft	1.3 m
Buoy mass	5736 kg
Translator mass	6240 kg
Generator damping	59 kN
Upper end-stop spring coefficient	776 kN/m
Upper end-stop spring length	0.6 m
Max stroke length upper/lower	1.8/1.8 m
Spring constant of connection line	300 kN/m

TABLE 2: THE TWO SEA STATES CONSIDERED IN THE PAPER. SIGNIFICANT WAVE HEIGHT H_s, PEAK PERIOD T_p, ENERGY PERIOD T_e

Sea State	H_s	T_p	T_e
1	5 m	8.2 s	7.5 s
2	7 m	11.7 s	10.1 s

To enable comparison with other studies regarding extreme forces on WECs, two sea states with the highest steepness used in [3] have been chosen for the present study. The extreme wave statistics are obtained from the Coastal Data Information Program 128 station and the National Data Buoy Center 46212 buoy near Humboldt Bay, California. The site represents one of the potential wave energy tests sites in the US. The selected extreme sea states are representative environments along the 100-year extreme wave contour, see Fig. 2 and Table 2.

Equivalent regular waves For the equivalent regular wave profile, the same methodology is applied as in [24]. The

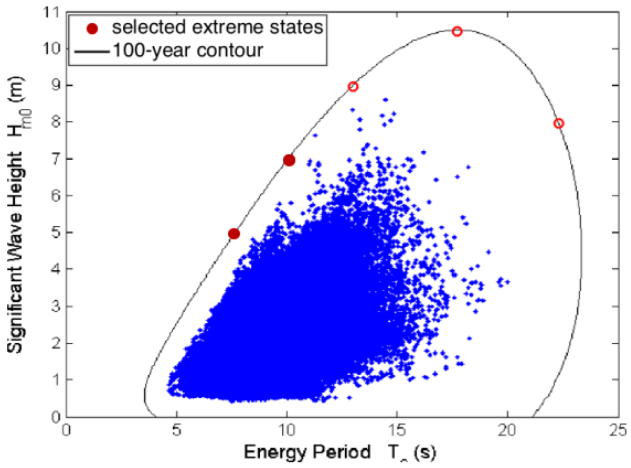

FIGURE 2: THE EXTREME SEA STATES HAVE BEEN CHOSEN FROM THE 100-YEAR CONTOUR AT THE HUMBOLDT BAY. SEA STATES MARKED WITH CIRCLES WERE USED ALSO IN [3], SEA STATES SELECTED FOR THE PRESENT PAPER SHOWN AS FILLED CIRCLES. FIGURE ADAPTED FROM [23].

TABLE 3: THE EQUIVALENT REGULAR WAVES OF TWO SEA STATES ARE CONSIDERED.WAVE HEIGHT H, PERIOD T AND STEEPNESS H/λ OF THE WAVES.

Sea State	$H = 1.9 \cdot H_s$	$T = T_p$	H/λ
1	9.5 m	8.2 s	0.091
2	13.3 m	11.7 s	0.065

irregular sea state can be represented by a regular wave with wave height $H = K \cdot H_s$, to approximate the maximum WEC responses, and period $T = T_p$. H_s and T_p are the significant wave height and peak period of the sea state, and $K = 1.9$. This value comes from the assumption that the extreme wave height follows a Rayleigh distribution and the maximum 100-year individual wave height H_{100} for sea states is most likely 1.9 times of the significant wave height for the 100-year wave (H_{s100}) assuming the storm lasts for 3 hours with 1000 waves [25]. In Table 3, the equivalent regular wave profiles can be found.

Equivalent focused wave Focused wave groups are used in physical and numerical studies to investigate the interaction of marine structures and ships with extreme waves. A focused wave is defined as the superposition of many smaller amplitude waves focusing at a preselected location and time using linear wave theory.

TABLE 4: THE EQUIVALENT FOCUSED WAVES OF TWO SEA STATES ARE CONSIDERED. STEEPNESS kA, MAX CREST AMPLITUDE A, PEAK PERIOD T_p, AND CHARACTERISTIC LENGTH L_c OF THE WAVES.

Sea State	kA	A	$T = T_p$	L_c
1	0.28	4.65 m	8.2 s	105 m
2	0.20	6.5 m	11.7 s	205 m

Different methods exist to design equivalent focused waves from a given irregular sea state. The most likely extreme response (MLER) method uses the linear response amplitude operator of a WEC and the wave spectrum to produce a wave profile that gives the largest device response. It was used in [3] for five extreme states along a 100-year wave contour and in [13] for two extreme waves along a 50-year contour.

In the NewWave Theory approach, the average shape of the highest wave with a specified exceedance probability is produced for a given sea state [26]. The theory has been used extensively to study WEC behaviour in equivalent extreme waves both numerically and experimentally, see, e.g., [5, 6, 11, 14, 16, 27]. In Table 4, the equivalent focused wave profiles can be found.

The theoretical amplitude of the maximum wave crest is set to be the largest expected amplitude in N waves,

$$A = \sqrt{2m_o \ln(N)} \tag{1}$$

where m_o is the zeroth spectral moment and $N = 1000$, representing the approximate number of waves expected in a 3 h sea state. The characteristic length, L_c, is based on the peak period, T_p, and for the crest steepness, kA, the peak wave number is used.

Numerical model

This paper presents numerical simulations performed using an advanced approach to model the highly non-linear interaction of extreme wave events with the floating point-absorber WEC. The Reynolds-Averaged Navier Stokes (RANS) equations are solved using a Finite Volume approach for two incompressible fluids using a Volume of Fluid (VoF) interface capturing scheme. The effect of turbulence is included through the use of a $k-\omega$ *SST* turbulence model and $y+$ wall treatment [28]. The open source CFD software OpenFOAM v.4.1 has been used for the numerical simulations. The fluid-structure interaction is implemented using the sixDoFRigidBodyMotion utility of the CFD code and for the solution the waveDyMFoam solver allowing dynamic mesh motion.

Boundary conditions for the quantities k and ω at the inlet are related to the celerity of the incoming wave as proposed by [29]. The simulation zone is specified with a length of $3 \cdot \lambda$, where λ is the wave length. In particular, the simulation zone has length $2 \cdot \lambda$ and $1 \cdot \lambda$ upstream and downstream of the WEC, respectively. Numerical wave generation and absorption is defined through relaxation zones. An additional length of $1 \cdot \lambda$ at the inlet and $2 \cdot \lambda$ at the outlet of the NWT is added. The relaxation zone method implemented in the waves2Foam toolbox is employed [30]. To support wave propagation without excessive wave damping, a band of refined cells around the free surface is applied. In the region close to the buoy, the mesh is more refined to capture the radiation, diffraction forces on the body and the fluctuations near the boundary layer accurately. Towards the outlet the mesh grading is used in the $x-$direction to decrease the computational cost. The depth is 70 m (in full scale) as in [3].

All the simulations have been done at a 1:20 scale, but the results are presented in full scale to allow for direct comparison with other publications. For point-absorbers, it was shown in [31] that scale effects are relatively small, but some uncertainty, especially in the surge response, is associated with the scaling of the results due to viscous effects. Two sea states are considered and modeled in terms of equivalent regular and equivalent focused waves. The significant wave height H_s and the peak period T_p of the sea states, as well as the characteristics of the equivalent regular and focused waves are shown in Tables 2-4.

Regular waves The regular waves are generated as Stokes 5th order waves with steepness (defined as H/λ) 0.091 and 0.065 for the sea state #1 and #2, respectively. A regular wave generated in the NWT is shown in Fig. 3 and the buoy size and position in relation to the NWT is shown in Fig. 4. The regular wave simulations were run for a duration of $15 \cdot T$ and adjustable time step with a Courant number of 0.25. The compression term C_α is set to 0.2 for keeping the effect of the artificial compression negligible, since the examined waves of this paper have high steepness. OpenFOAM uses an artificial compression term in the phase-fraction equation, which is introduced to keep the air-water interface sharp. For increasing surface curvature, the term also introduces increasing damping on the wave amplitude [15]. OpenFOAM uses an artificial compression term in the phase-fraction equation, which is introduced to keep the air-water interface sharp. For increasing surface curvature, the term also introduces increasing damping on the wave amplitude [15].

Focused waves For the focused wave simulations, the same sea states are examined with steepness 0.076 and 0.047 for the sea state #1 and #2, respectively. The wave steepness, $k \cdot A$, is defined as the maximum crest amplitude for the peak wave period number [32]. The numerical wave tank width and depth are the same as for the case of regular wave simulations. The 31 m

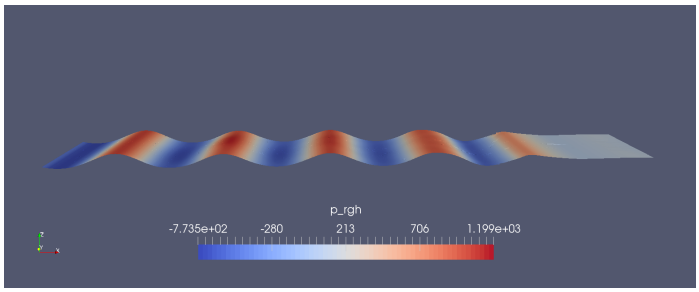

FIGURE 3: A REGULAR WAVE PRODUCED IN THE NUMERICAL WAVE TANK.

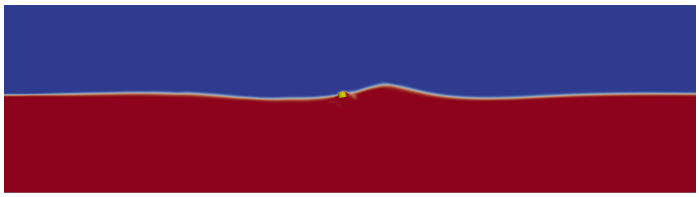

FIGURE 4: TWO-DIMENSIONAL VIEW OF THE CYLINDER BUOY IN THE NUMERICAL WAVE TANK.

long ($0 \leq x \leq 31$) computational domain (corresponding to 620 m full scale) is adjusted so that there is roughly two wavelengths or greater for the outlet relaxation zone downnstream the WEC. The length of the inlet relaxation zone is kept short (1m, which is equal to $L_c/100$ and $L_c/200$ for #1 and #2 sea state respectively), since previous studies indicate that the model is not overly sensitive to this value [32]. The WEC buoy is positioned at x = 4.35 m and y = 0 m, and the geometric characteristics are presented in the Table 1.

The NewWave theory wave components were applied using first order waves superposition. The number of wave components required to define a specified wave within a given tolerance level has to be determined. In [32], the maximal number of components N was set to 100, since instabilities have been shown to appear for large N. In this paper, a comparison has been made for 65, 85 and 100 wave components, with the same resulting focused wave. Therefore, the number of components has been set to 65. The superposition of wave phases was specified at focus time $t_f = 8$ s (35.8 s full scale) and the wave components focusing at the WEC location. The buoy had zero initial displacement and velocity.

The discretization in the water surface region, ($-2 \cdot H_s \leq$ z $\leq 2 \cdot H_s$) is set to $H_s/\Delta z = 20$ m, determined using a mesh convergence study as discussed later in the paper. The aspect ratio is 1 close to water surface, however, to reduce the computational cost, mesh grading is applied in the x-direction (x > 15 m) and z-direction ($|z| > 5 \cdot H_s$). The snappyHexMesh technique is applied to form the mesh around the WEC which has one level

higher grid refinement compared to water surface region. For solving the physics of the flow in the near wall region, the wall functions technique is applied. Since the first cell center needs to be placed in the log-law region, the $y+$ should be with in the range $30 < y+ < 200$, which is satisfied in the simulations. The final mesh size is approximately 16 and 13 million cells in both cases respectively.

RESULTS

Validation and mesh convergence

The OpenFOAM model used in this paper has been used previously in [12,21,22] to study the dynamics of a similar wave energy converter in different extreme wave conditions. In [12, 21], the numerical model was validated with experimental data from wave tank tests of a 1:20 scale WEC model, subject to extreme focused waves embedded in a regular wave background.

Regular waves To apply the model for the wave conditions considered in this paper, a mesh convergence study has been carried out to validate the reliability of the numerical simulations. For a monochromatic sea state, the mesh resolution of the NWT is evaluated by comparing the generated wave height against theory. The mesh convergence study is presented by running the first sea state regular wave case with five different meshes of increasing size. To determine the required resolution, the wave is run on a series of 2D meshes. In this work the aspect ratio is 1 close to the water surface, however towards the outlet the mesh is getting coarser in the x-direction to decrease the computational cost. The resolution in z-direction is expressed as number of cells per wave height; 8, 10, 12, 15, 20 cells/H.

The evaluation metrics for the generated wave height are i) the mean wave height $\bar{H}$, ii) standard deviation σ, iii) the relative error ε of the average wave height and the desired theoretical value H_{theory}. The mean wave height $\bar{H}$ is calculated following the procedure described in the publication [33] and expressed as:

$$\bar{H} = \frac{1}{j}\sum_{j=i_1}^{i_1+j} H_j(x) \tag{2}$$

where several periods $j \in [i_1, i_1 + j]$ are used and H_j is the wave height for each period. The wave gauge located in the future buoy position is used to measure the wave height for 4 periods. The standard deviation and relative error are defined as

$$\sigma = \sqrt{\frac{\sum_{j=i_1}^{i_1+j}(H_j - \bar{H})^2}{j-1}}, \tag{3}$$

$$\varepsilon = \left| \frac{\bar{H} - H_{\text{theory}}}{H_{\text{theory}}} \cdot 100\% \right|. \tag{4}$$

TABLE 5: MESH CONVERGENCE FOR THE EQUIVALENT REGULAR WAVE OF SEA STATE 1.

Cells/H_s	$\bar{H}$	σ	ε
8	0.4694	0.00109	1.8613
10	0.4718	0.00083	1.0550
12	0.4728	0.00059	0.7206
15	0.4732	0.00044	0.5709
20	0.4734	0.00011	0.5645

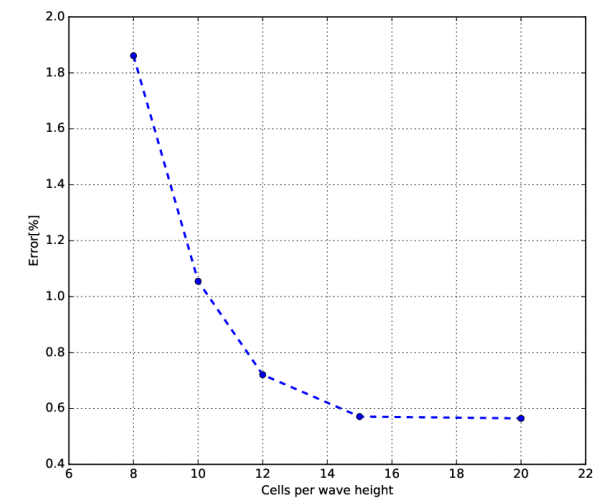

FIGURE 5: MESH CONVERGENCE FOR THE EQUIVALENT REGULAR WAVE OF SEA STATE 1.

The results of the mesh convergence study for the regular wave are shown in Fig. 5 and Table 5, and show good accuracy for all five mesh cases with an error within 2%. Based on this, the second finest mesh resolution was chosen for the remainder of the study. This is translated as a resolution close to water surface of $\Delta x = \Delta y = \Delta z = 0.95$ m and 1.33 m for sea state #1 and #2, respectively.

Focused waves A mesh convergence study has been conducted also for the focused waves, generated using 65 wave components. To determine the required resolution, five cases with a 2D uniform mesh of increasing resolution have been used. The finer mesh is considered as the reference case and the percentage difference between one mesh and the reference case is plotted in Fig. 6. To determine the discretization, three criteria measured at the focus location are considered: a) peak height, b)

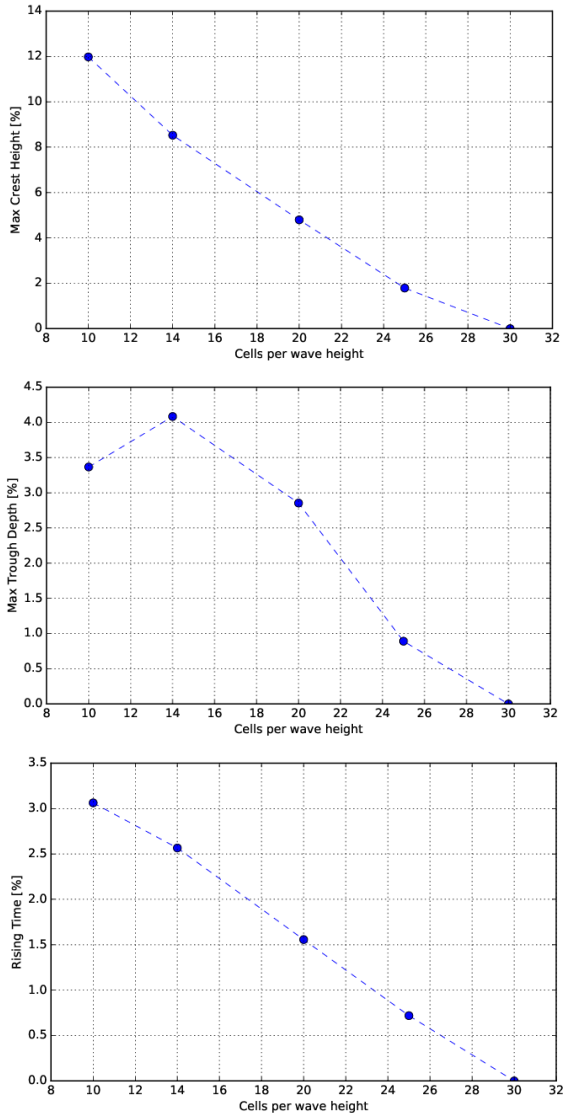

FIGURE 6: MESH CONVERGENCE FOR THE EQUIVALENT FOCUSED WAVES OF SEA STATE 1.

maximum trough depth c) rising time. An initial user-specified tolerance of 3% in each of the criterion is imposed. For the maximum peak height, this criterion is fulfilled for the finer cases, but the maximum trough depth and rising time converge already at the quite coarse mesh resolutions. As a compromize between mesh convergence and computational cost, a final mesh discretization of 20 cells/H_s is chosen. This is translated as a resolution of $\Delta x = \Delta y = \Delta z = 0.25$ m and 0.35 m for sea state #1 and #2, respectively. The generated focused wave for sea state #1 is shown in Fig. 7.

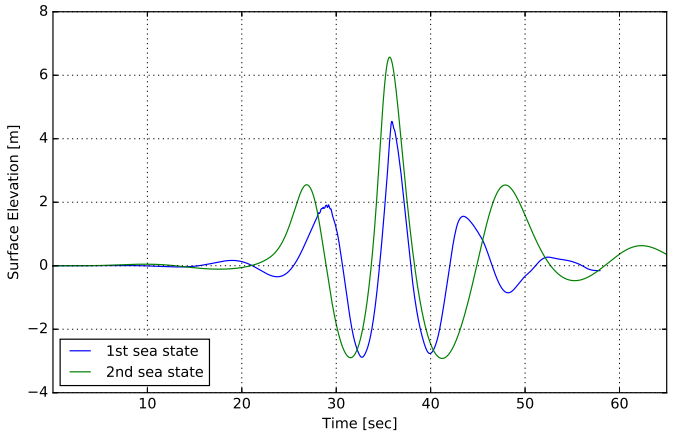

FIGURE 7: SURFACE ELEVATION OF EQUIVALENT FOCUSED WAVE OF SEA STATE 1 AND 2.

Dynamics in extreme wave events

The dynamics of the buoy in heave, pitch, and surge in the equivalent regular waves of sea states #1 and #2 are shown in Fig. 10. As can be seen from the figures, the heave displacement is constrained by the stroke length of the generator. In sea state #1, the heave motion is smooth during the first three regular wave periods, and the translator hits the upper end-stop spring in the fourth period ($t = 17$ s, highlighted by a vertical black dashed line) and onwards, justifying the sharp peaks in the plot. In sea state #2, the upper end-stop is hit in each wave period. As sea state #2 has a 40% higher wave height, it can be expected that the heave motion is more pronounced, which is also seen a 25% increase in the results. The pitch motion follows the heave response. In particular, the minimum pitch motion happens at the same time as the minimum heave displacement, whereas during the maximum heave displacement, the pitch motion is oscillating between positive and negative values. The limited stroke length also affects the pitch motion, once the upper end-stop is hit, the range of oscillation is increasing. Overall, the buoy's pitch motion is mainly anticlockwise (negative) and the peak values are connected to the wave troughs and crests. For the sea state #1, where the wave height is lower, the pitch motion reaches greater peak values. For both sea states, the surge motion is first seen to drift, until a rather stable oscillation around an equilibrium mean position is obtained. The surge displacement is increased after some periods and tends to remain in that high level. In Fig. 8 and 9, the visualization of the buoy motion in regular wave trains is illustated with the grey buoy being at the inital position and the yellow buoy following the wave propagation. For both sea states, the surge displacement dominates during the whole simulation, whereas the heave displacement is restricted due to the stoke lenght of the translator and the extensive surge motion.

Fig. 7 shows the predicted surface elevation of the focused

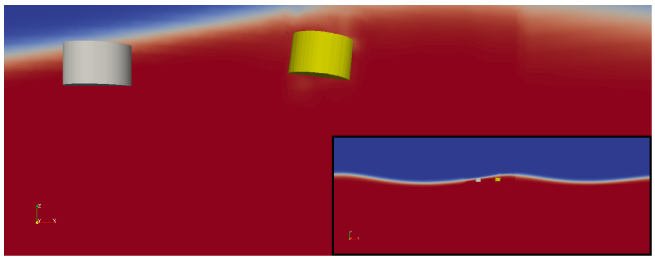

(a) Maximum surge response ($t = 110$ s)

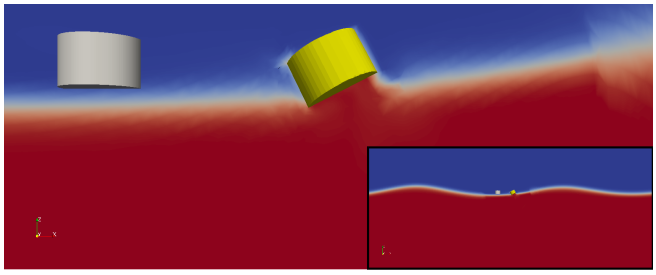

(b) Minimum heave response ($t = 112$ s)

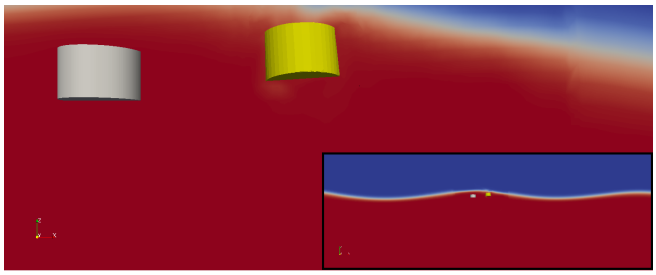

(c) Maximum heave response ($t = 116$ s)

FIGURE 8: CONTOURS OF THE VOLUME FRACTION OF WATER FOR REGULAR WAVE, SEA STATE 1.

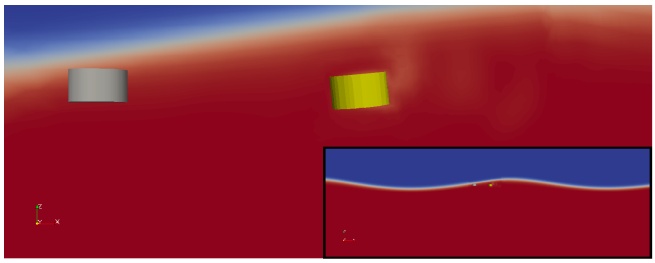

(a) Maximum surge response ($t = 121$ s)

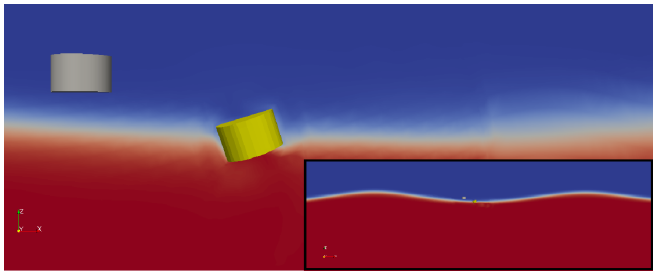

(b) Minimum heave response ($t = 125$ s)

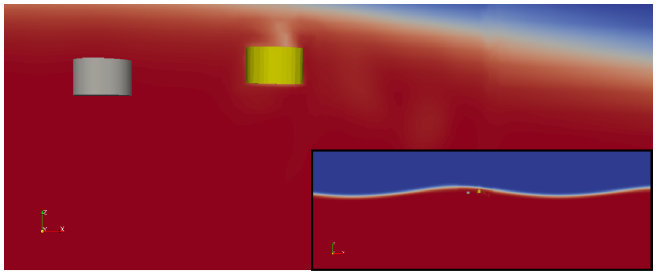

(c) Maximum heave response ($t = 130$ s)

FIGURE 9: CONTOURS OF THE VOLUME FRACTION OF WATER FOR REGULAR WAVE, SEA STATE 2.

waves at the target location in an empty numerical wave tank for both the examined sea states. The wave is focusing at $t_f = 35.8$ s. As expected the sea state #2 has greater peak height but the rising time is decreased with increasing steepness, due to the increase in peak frequency [32]. In the present work the focused wave in the sea state #1 and #2 do not break, in contrast to the prediction in [3], that the chosen waves would lie within the breaking wave limit.

The buoy motion in the equivalent focused waves is illustrated for three time instances in Fig. 11, and shown for the full time range in Figs. 12 and 13. The heave response is connected to the surface elevation, therefore the focused wave profile with higher maximum crest amplitude drives the buoy to higher heave displacement. The maximum heave response occurs prior to the instant of maximum wave elevation and the translator hits the end-stop spring of the generator in the regions I and II as defined by the vertical dashed lines in the heave plots. For the milder sea state #1, the upper end-stop spring is hit only when the wave is focusing, whereas in sea state #2 the spring is hit twice. At the beginning of the simulation, for both sea states, the surge response is limited but after the focusing time, $t_f = 35.8$ s, the buoy behaves as a wave follower due to limited restraint acting on the floating buoy horizontally. The pitch motion reaches the peaks a few seconds before and after the focusing time but the moment of wave focusing the pitch response is almost zero for both sea states.

Comparing the regular and focused wave profiles, the heave displacement is higher for the latter case for both sea states. Once the translator exceeds the free stroke length limit of 1.2 m, the upper end-stop spring is compressed and once reached the limit of 1.8 m, the spring is fully compressed. As can be noticed by observing the heave response in regular waves (Fig. 10, the value is always less than 1.2 m even when the end-stop spring is hit. At the same time, it is worth noticing the surge displacement of

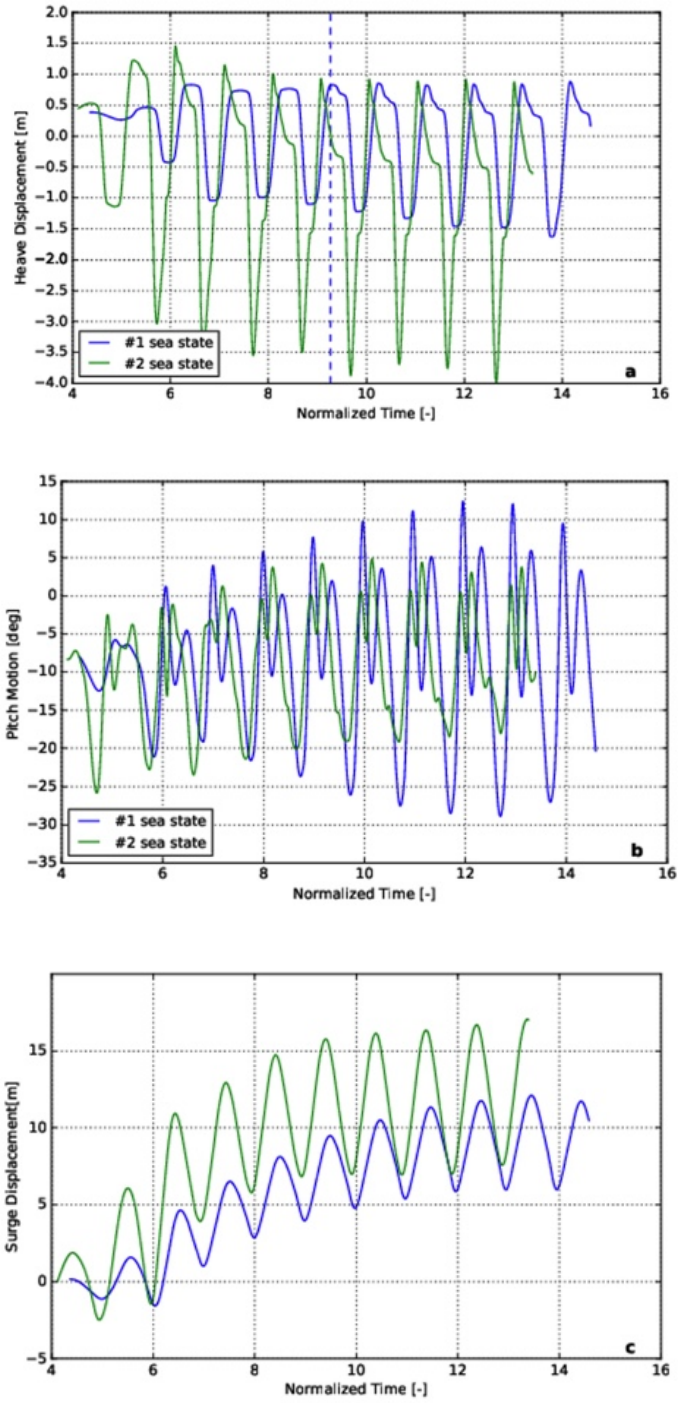

FIGURE 10: BUOY DYNAMICS IN EQUIVALENT REGULAR WAVES OF SEA STATES 1 AND 2.

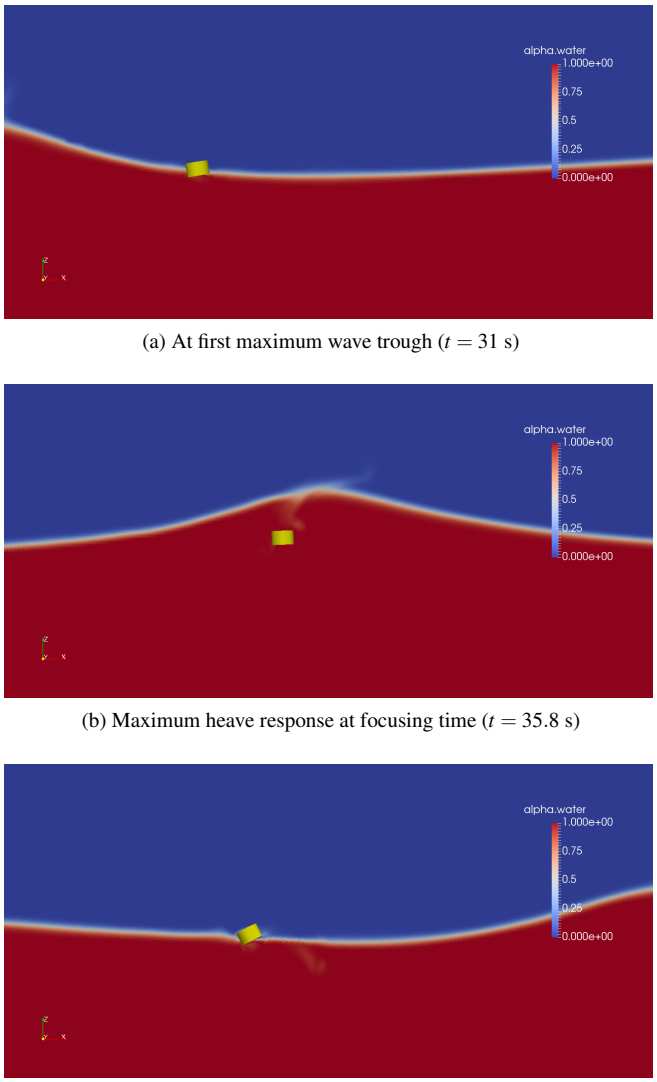

(a) At first maximum wave trough ($t = 31$ s)

(b) Maximum heave response at focusing time ($t = 35.8$ s)

(c) Minimum heave response ($t = 40$ s)

FIGURE 11: CONTOURS OF THE VOLUME FRACTION OF WATER FOR FOCUSED WAVES, SEA STATE 2.

the buoy, which is high and the displacement of the translator does not match with the heave response of the buoy due to the large surge response. On the other hand, for the case of the focused wave trains, the surge motion is limited especially before the focusing time, $t_f = 35.8$ s, and the heave response of the buoy follows the displacement of the translator. After the focusing time, the surge motion increases resulting in the restriction of the heave motion even though the translator continues hitting the upper end-stop spring. The high surge response in regular waves can be explained since the continuous wave trains interacting with the buoy, pushing it further and not allowing to it recover its initial position. In terms of focused waves, the instantaneous behaviour of the wave train does not allow the continuation of the same phenomenon. The pitch response reaches higher peaks for the focused wave profile but in general the pitch oscillation

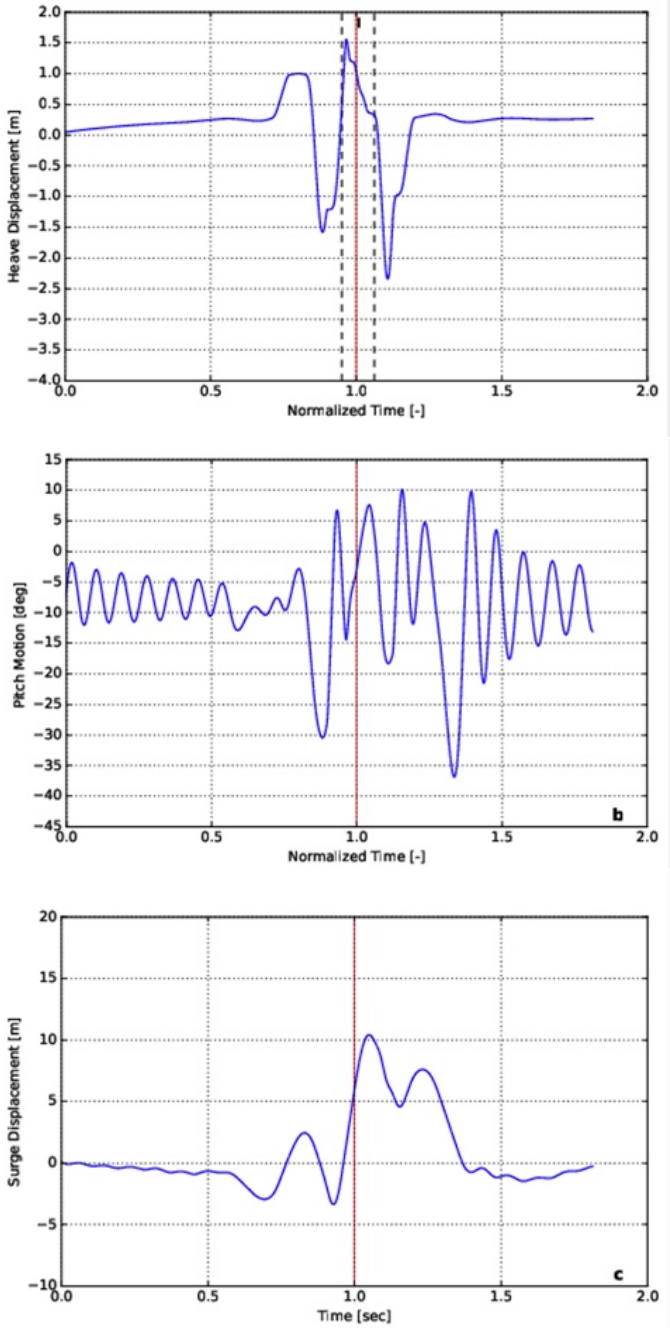

FIGURE 12: BUOY DYNAMICS IN EQUIVALENT FOCUSED WAVE OF SEA STATE 1.

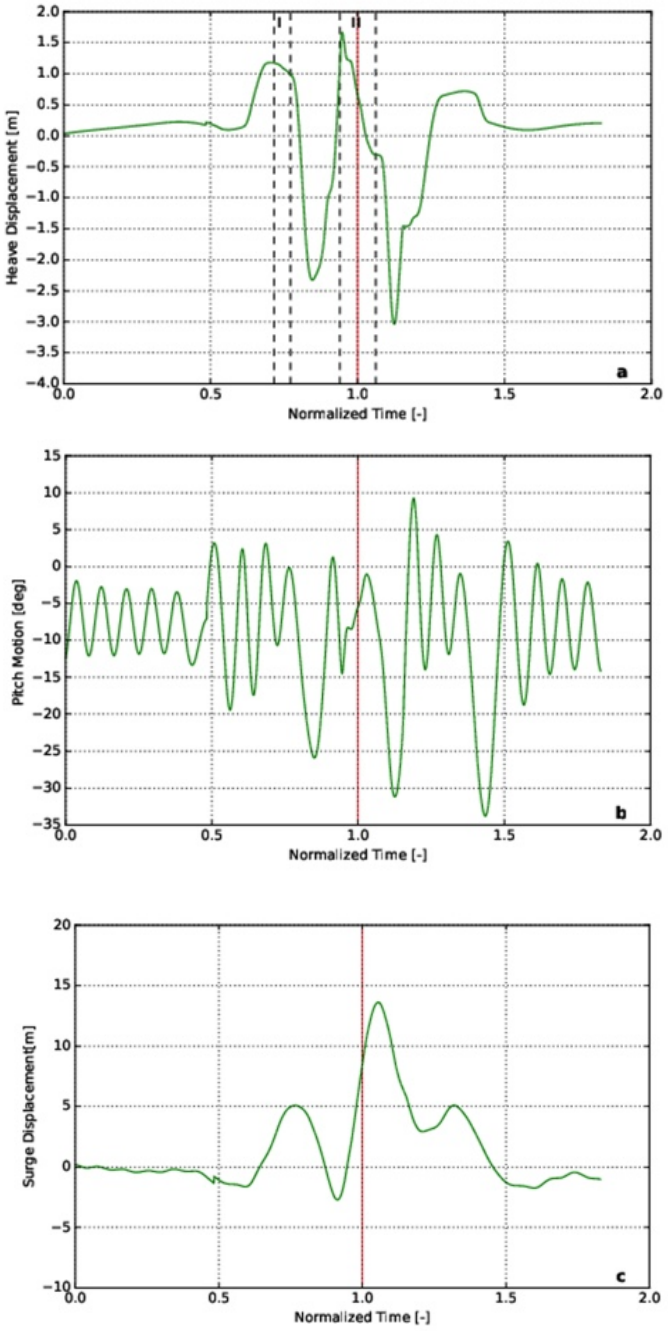

FIGURE 13: BUOY DYNAMICS IN EQUIVALENT FOCUSED WAVE OF SEA STATE 2.

range is greater for the regular waves. In general, the dynamics are different for the focused and regular wave profiles since the regular wave train interacts with the buoy for a longer time allowing the development of dynamic phenomena. On the other hand, the focused wave simulations provide the critical instantaneous response leading to the fact that an embedded focused wave train would be a more realistic approach for the extreme waves investigation. This supports the conclusions [5] and [3], where it has been concluded that focused waves can be less accurate when the

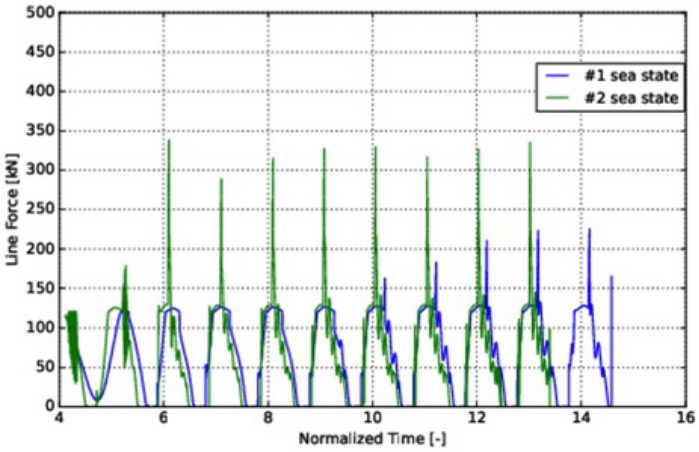

FIGURE 14: LINE FORCE IN EQUIVALENT REGULAR WAVE OF SEA STATE 1 AND 2.

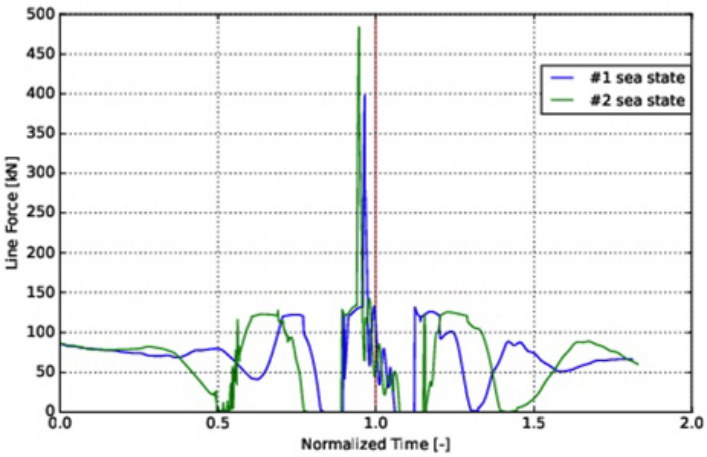

FIGURE 15: LINE FORCE IN EQUIVALENT FOCUSED WAVE OF SEA STATE 1 AND 2.

load response depends heavily on the instantaneous wave train.

Extreme loads

The line forces acting on the WEC in regular and focused waves are shown in Fig. 14 and Fig. 15 respectively. The forces are dominated by the heave displacement as expected, but are also affected by the surge offset of the buoy. The force plateaus are around 130 kN in each cycle, which corresponds to the full submergence of the buoy. As the wave crest passes, the force slowly varies with the dynamic component of the wave pressure and centripetal force due to surge motion. In the later cycles of sea state #1 and in almost all cycles of sea state #2 of the regular waves in Fig. 14, a secondary peak force occurs. This happens when the translator exceeds its allowed stroke length and hits the upper end-stop spring. Hence, the magnitude of the survival force is governed by the stiffness of the end stop spring and the translator velocity when it hits it. The larger amplitude and longer period time of sea state #2 results in larger velocity, heave displacement and consequently force response. Please also note that the mooring line goes slack in almost all of the cycles simulated, indicating that the waves move faster than the free fall of the translator subject to the damping force.

Interestingly, both heave displacement and line forces are significantly higher in the focused wave scenario compared with the equivalent regular waves. The focused wave peak line force increases with 78 % and 48 % for sea state #1 and #2 respectively, and the corresponding increase in heave is approximately 76 % and 33 %.

DISCUSSION AND CONCLUSIONS

In this paper, the dynamics and line forces of a point-absorber wave energy converter has been studied using a CFD model in extreme waves. Two sea states along the 100-year wave contour at Humboldt Bay, California have been chosen for the study, and are modelled both as equivalent regular and equivalent focused waves using NewWave theory. The wave energy converter consists of a floating cylinder buoy connected to a direct-driven linear generator with limited stroke length.

The design-wave approaches of regular and focused waves reveal that the dynamics and extreme loads on the floating buoy differ in the differently modeled extreme waves. The examined sea states are characterized by high steepness, but the breaking limit of $H/\lambda = 0.14$ is not exceeded. This is confirmed by the simulations as there is no occurrence of breaking waves, although it should be kept in mind that breaking waves is generally not well captured by the VoF method. Observing the Fig. 8, 9, 11, the high steepness drives the buoy to be either fully submerged or partially out of the water, suggesting the importance of non-linear methods to study the response in extreme waves.

Important part of the present work is the comparison with [3], in which focused design-wave approach is applied using the MLER method for both sea states examined here. As in [3], we can conclude that the high steepness mainly affects the heave and pitch motion of the buoy. The amplitude of the device response is reduced for steep and short period focused waves. The pitch response is maximum for the sea state #1, which has the steepest focused wave. Moreover, for the focused waves simulations, the peak heave displacement and peak line force appear some seconds before the maximum crest elevation, as shown in the Fig. 12a, 13a and 15. Also, our results show that the commonly used assumption of buoy motion only in heave might lead to erroneous conclusions on the dynamics and loads. This supports the findings in [3], where it was concluded that different predictions for the response in extreme waves were obtained if the buoy was allowed to move in more degrees of freedom, than

if it was restricted to heave only.

The end stop forces shown in Figs. 14 and 15 show how the device should be designed in order to survive the extreme loads in the studied wave conditions. The overtopping of the device introduces dynamics that cannot be well captured by linear methods. These results should be considered relative to the damping coefficient used in the simulations. With a relatively high value of damping such as was used in this case, the translator get a slow response, resulting in long periods of slack in the wave troughs and in a limited vertical velocity during the wave crests which means limited peak forces, which has been confirmed in wave tank experiments in [6]. Please note that the dynamics of the mooring line and the inertial forces of the translator are not taken into account in the present model, both of which are interesting parameters to consider for a deeper analysis of the line slack period and the ensuing snap load in the line.

Although the maximum surge displacement is slightly smaller in the focused waves compared with the regular case, the surge velocity is significantly larger in the focused waves. In both the focused wave sea states, the displacement of the device is 10.5 m and 13 m over one wave period, while the regular waves surge equivalence is in the range of 6 m and 9.5 m. This represents a very clear difference between the buoy dynamics in focused and in regular survival waves and highlights the importance of the wave grouping and the motion history of the buoy for the peak force and the dynamic response of a device, which is in line with what has been previously reported [3, 5].

Another uncertainty stems from the derivation of the 50-year recurrence wave conditions. Whereas wave buoys only provide point observations and tend to underestimate very large individual waves [34], spectral wave models typically underestimate extreme significant wave heights due to their inability to resolve high-energy wind gusts to a fine resolution. Although the extreme wave statistics can be improved with various methods (see, e.g., [35]), this remains an uncertainty of all survivability studies based on extreme wave statistics.

ACKNOWLEDGMENT

The research in this paper was supported by the Centre of Natural Hazards and Disaster Science, Sweden, the Swedish Research Council (VR, grant number 2015-04657), the Swedish Energy Authority (project number 47264-1), the PRIMaRE Short Research Visit Grant (SRV). This scientific paper was also supported by the Onassis Foundation, scholarship ID: F ZP 021-1/2019-2020.

The CFD simulations were performed on resources provided by the Swedish National Infrastructure for Computing (SNIC) at two HPC clusters: Uppsala Multidisciplinary Center for Advanced Computational Science (UPPMAX) and Tetralith at the National Supercomputer Centre, Linköping University.

REFERENCES

[1] Starling, M., 2009. Guidelines for reliability, maintainability and survivability of marine energy conversion systems: marine renewable energy guides. Tech. rep., European Marine Energy Centre.

[2] Coe, R. G., Neary, V. S., Lawson, M., Yu, Y., and Weber, J., 2014. Extreme conditions modeling workshop report. Tech. rep., National Renewable Energy Lab (NREL), USA.

[3] Quon, E., Platt, A., Yu, Y.-H., and Lawson, M., 2016. "Application of the most likely extreme response method for wave energy converters". In ASME 2016 35th Int. Conf. on Ocean, Offshore and Arctic Engineering, American Society of Mechanical Engineers.

[4] Van Rij, J., Yu, Y.-H., and Coe, R. G., 2018. "Design load analysis for wave energy converters". In ASME 2018 37th Int. Conf. on Ocean, Offshore and Arctic Engineering, American Society of Mechanical Engineers.

[5] Hann, M., Greaves, D., and Raby, A., 2015. "Snatch loading of a single taut moored floating wave energy converter due to focussed wave groups". *Ocean Engin.,* ***96***, p. 258.

[6] Göteman, M., Engström, J., Eriksson, M., Hann, M., Ransley, E., Greaves, D., and Leijon, M., 2015. "Wave loads on a point-absorbing wave energy device in extreme waves". *Journal of Ocean and Wind Energy,* ***2***(3), pp. 176–181.

[7] Mackay, E., 2017. "Return periods of extreme loads on wave energy converters". In Proc. of the 12th European Wave and Tidal Energy Conference (EWTEC).

[8] Commission, I. E., 2016. Marine energy – wave, tidal and other water current converters. Part 2: Design requirements for marine energy systems. IEC TS 62600-2:2016-08. Tech. rep., IEC, Geneva, Switzerland.

[9] Coe, R., Yu, Y.-H., and Van Rij, J., 2018. "A survey of WEC reliability, survival and design practices". *Energies,* ***11***(1), p. 4.

[10] Ochi, M. K., 2005. *Ocean waves: the stochastic approach*, Vol. 6. Cambridge University Press.

[11] Ransley, E., Greaves, D., Raby, A., Simmonds, D., and Hann, M., 2017. "Survivability of wave energy converters using CFD". *Renewable Energy,* ***109***, pp. 235–247.

[12] Engström, J., Sjökvist, L., Göteman, M., Eriksson, M., Hann, M., Ransley, E., Greaves, D., and Leijon, M., 2017. "Buoy geometry and its influence on survivability for a point absorbing wave energy converter: Scale experiment and CFD simulations". In Proc. of the Marine Energy Technical Symposium (METS).

[13] Rosenberg, B. J., Mundon, T. R., Coe, R. G., Quon, E. W., Chartrand, C. C., Yu, Y.-H., and van Rij, J., 2019. "Development of WEC design loads: A comparison of numerical and experimental approaches". In Proc. of the 13th European Wave and Tidal Energy Conference (EWTEC).

[14] van Rij, J., Yu, Y.-H., and Tom, N., 2019. "Validation of simulated wave energy converter responses to focused

waves for CCP-WSI blind test series 2". In Proc. of the 13th European Wave and Tidal Energy Conference (EWTEC).

[15] Ransley, E. J., 2015. "Survivability of wave energy converter and mooring coupled system using CFD". PhD thesis, University of Plymouth, UK.

[16] Rafiee, A., and Fiévez, J., 2015. "Numerical prediction of extreme loads on the CETO wave energy converter". In 11th European Wave and Tidal Energy Conference (EWTEC). Nantes, France.

[17] Coe, R. G., Rosenberg, B. J., Quon, E. W., Chartrand, C. C., Yu, Y.-H., van Rij, J., and Mundon, T. R., 2019. "CFD design-load analysis of a two-body wave energy converter". *J. of Ocean Engin. and Marine Energy,* ***5***(2), pp. 99–117.

[18] van Rij, J., Yu, Y.-H., Guo, Y., and Coe, R. G., 2019. "A wave energy converter design load case study". *Journal of Marine Science and Engineering,* ***7***(8), p. 250.

[19] Waters, R., Stålberg, M., Danielsson, O., Svensson, O., Gustafsson, S., Strömstedt, E., Eriksson, M., Sundberg, J., and Leijon, M., 2007. "Experimental results from sea trials of an offshore wave energy system". *Applied Physics Letters,* ***90***(3), p. 034105.

[20] Leijon, M., Waters, R., Rahm, M., Svensson, O., Bostrom, C., Stromstedt, E., Engstrom, J., Tyrberg, S., Savin, A., Gravrakmo, H., et al., 2008. "Catch the wave to electricity". *IEEE Power and Energy Magazine,* ***7***(1), pp. 50–54.

[21] Sjökvist, L., Wu, J., Ransley, E., Engström, J., Eriksson, M., and Göteman, M., 2017. "Numerical models for the motion and forces of point-absorbing wave energy converters in extreme waves". *Ocean Engin.,* ***145***, pp. 1–14.

[22] Sjökvist, L., and Göteman, M., 2019. "Peak forces on a point absorbing wave energy converter impacted by tsunami waves". *Renewable energy,* ***133***, pp. 1024–1033.

[23] Dallman, A. R., and Neary, V. S., 2014. Characterization of US wave energy converter (WEC) test sites: A catalogue of met-ocean data. Tech. rep., Sandia National Lab.(SNL-NM), Albuquerque, NM (United States).

[24] Yu, Y.-H., Van Rij, J., Coe, R., and Lawson, M., 2015. "Preliminary wave energy converters extreme load analysis". In ASME 2015 34th Int. Conf. on Ocean, Offshore and Arctic Engineering, American Society of Mechanical Engineers.

[25] DNV (Det Norske Veritas), 2010. DNV-RP-C205 Environmental conditions and environmental loads. Tech. rep.

[26] Tromans, P. S., Anaturk, A. R., Hagemeijer, P., et al., 1991. "A new model for the kinematics of large ocean waves-application as a design wave". In The First International Offshore and Polar Engineering Conference, International Society of Offshore and Polar Engineers.

[27] Stallard, T., Weller, S., and Stansby, P., 2009. "Limiting heave response of a wave energy device by draft adjustment with upper surface immersion". *Applied Ocean Research,* ***31***(4), pp. 282–289.

[28] Menter, F. R., 1994. "Two-equation eddy-viscosity turbulence models for engineering applications". *AIAA journal,* ***32***(8), pp. 1598–1605.

[29] Lin, P., and Liu, P. L.-F., 1998. "A numerical study of breaking waves in the surf zone". *Journal of fluid mechanics,* ***359***, pp. 239–264.

[30] Jacobsen, N. G., Fuhrman, D. R., and Fredsøe, J., 2012. "A wave generation toolbox for the open-source CFD library: Openfoam®". *International Journal for numerical methods in fluids,* ***70***(9), pp. 1073–1088.

[31] Palm, J., Eskilsson, C., Bergdahl, L., and Bensow, R., 2018. "Assessment of scale effects, viscous forces and induced drag on a point-absorbing wave energy converter by CFD simulations". *J. of Marine Science and Engin.,* ***6***(4), p. 124.

[32] Brown, S. A., Ransley, E. J., and Greaves, D., 2019. "CCP-WSI blind test series 2: Assessment of focused wave impacts on floating WECs using openFOAM". In Proc. of the 13th European Wave and Tidal Energy Conference (EWTEC).

[33] Windt, C., Davidson, J., Schmitt, P., and Ringwood, J. V., 2017. "Assessment of numerical wave makers". In Proc. of the 12th European Wave and Tidal Energy Conference.

[34] Alves, J. H. G., and Young, I. R., 2003. "On estimating extreme wave heights using combined Geosat, Topex/Poseidon and ERS-1 altimeter data". *Applied Ocean Research,* ***25***(4), pp. 167–186.

[35] Neary, V. S., Seng, B., Yang, Z., Allahdadi, N., He, R., and Wang, T., 2019. "Model performance predicting extreme wave heights for project risk assessment and WEC design". In Proc. of the 13th European Wave and Tidal Energy Conference (EWTEC).